Carbohydrate Polymers 87 (2012) 1091–1097

Contents lists available at SciVerse ScienceDirect

Carbohydrate Polymers

journal homepage: www.elsevier.com/locate/carbpol

Purification and characterization of chitin deacetylase from *Penicillium oxalicum* SAE_M-51

Nidhi Pareek, V. Vivekanand[1], Samta Saroj, Ashwani K. Sharma, Rajesh P. Singh*

Department of Biotechnology, Indian Institute of Technology Roorkee, Roorkee 247667, India

ARTICLE INFO

Article history:
Received 1 June 2011
Received in revised form 12 August 2011
Accepted 16 August 2011
Available online 22 August 2011

Keywords:
Penicillium oxalicum
Chitin deacetylase
Purification
Kinetics
Thermodynamic parameters
Circular dichroism

ABSTRACT

Chitin deacetylase (CDA) with a molecular mass of 53 kDa was purified from *Penicillium oxalicum* SAE_M-51. Optimal temperature and pH of the purified enzyme were 50 °C and 9.0 respectively. Activation energy ($E_{a,d}$), free energy (ΔG^*_d), enthalpy (ΔH^*_d) and entropy (ΔS^*_d) for enzyme denaturation at optimal temperature were 114.72 kJ mol^{-1}, 97.86 kJ mol^{-1}, 112.04 kJ mol^{-1}, 43.93 J mol^{-1} K^{-1}, respectively. Enzyme had the half life of 693.10 min at its optimum temperature. It had notably deacetylated glycol chitin and chitin oligomers having degree of polymerization of more than four. Increased enzyme activity was observed with metal ions mainly Cu^{2+} and Co^{2+}. No inhibition of the enzyme was observed by the end product i.e. acetate (0–60 mM). Far-UV CD spectroscopic analysis revealed presence of 56.26% α and 15.63% β-helical structures. Significant homology of the enzyme was observed with CDAs from fungal and yeast strains.

1. Introduction

Chitin, a polymer of β-(1,4) linked *N*-acetyl glucosamine subunits is one of the most abundant biomass polysaccharide on earth after cellulose. This vastly available biopolymer still remains industrially unexploited because of its higher degree of crystallinity and insolubility in most of the solvents. Deacetylation of chitin either by chemical or biological means leads to the production of chitosan, a polymer of β-(1,4) linked glucosamine residues with some unique properties like biodegradability, biocompatibility, non-toxicity, solubility in acidic solutions, which makes it a polymer of interest for an array of industrial applications such as pharmaceutics, food, agriculture, tissue engineering, and cosmetics (Aranaz et al., 2009). Bioconversion of chitin to chitosan can be achieved by using chitin deacetylase (CDA, EC 3.5.1.41), which catalyzes deacetylation of *N*-acetyl-D-glucosamine residues in mild reaction conditions and results into superior quality chitosan. The enzyme is a member of carbohydrate esterase (CE) family 4 (http://afmb.cnrs-mrs.fr/CAZY/) (Caufrier, Martinou, Dupont, & Bouriotis, 2003). CDA was initially identified and partially purified from the mycelial extracts of *Mucor rouxii* by Araki and Ito (1975), since then, presence of the enzyme has been detected in several other fungi viz. *Colletotrichum lindemuthianum* (Tsigos & Bouriotis, 1995), *Gongronella butleri* (Maw, Tan, Khor, & Wong, 2002), *Metarhizium anisopliae* (Nahar, Ghormade, & Deshpande, 2004), *Scopulariopsis brevicaulis* (Cai et al., 2006), *Mortierella* sp. DY-52 (Kim, Zhao, Oh, Nguyen, & Park, 2008), etc. and also in few bacterial species viz. *Clostridium aminovalericum* (Simunek et al., 2004), *Vibrio parahaemolyticus* KN1699 (Kadokura et al., 2007), etc. Most of the strains observed so far are intracellular producers with lower activity and yield, which is a serious limitation for the bioconversion process.

Enzyme production, characterization and application are an enduring, fundamental and vital area of current research. The potential and biotechnological significance of CDA is due to its role in the chitin deacetylation. So, it would be pertinent to look for novel extracellular CDA producers, which may result into remarkably higher levels of CDA. Further, the CDA thus obtained preferably should be stable under standard conditions of pH, temperature, etc. that may therefore affect into higher yields of the end product. Further, study of enzyme kinetics and thermodynamic parameters would provide information about the factors affecting thermal denaturation of the enzyme.

In the present investigation, an extracellular CDA from the mutant *Penicillium oxalicum* SAE_M-51 was purified to homogeneity. Kinetic parameters of the enzyme were also evaluated using various chitinous substrates. Thermodynamic parameters that regulate the irreversible inactivation of the enzyme had also been analyzed. The present study would therefore help decipher the

* Corresponding author. Tel.: +91 1332 285792; fax: +91 1332 273560.
E-mail address: rpsbsfbs@iitr.ernet.in (R.P. Singh).
[1] Present address: Protein Engineering and Proteomics Group, Department of Chemistry, Biotechnology and Food Sciences, Norwegian University of Life Sciences, Ås 1430, Norway.

0144-8617/$ – see front matter © 2011 Elsevier Ltd. All rights reserved.
doi:10.1016/j.carbpol.2011.08.041

characteristic features of the CDA that appears to be compatible for industrial exploitation of the enzyme for bioconversion reactions.

2. Materials and methods

2.1. Microorganism

P. oxalicum SAE_M-51 was developed in our laboratory from the wild type *P. oxalicum* ITCC 6965, isolated from residual materials from sea food processing industry (Saubhagya Seafoods, Porbandar Gujarat, India) following successive stages of mutagenesis using microwave irradiation and ethidium bromide (EtBr) (Pareek, Vivekanand, Dwivedi, & Singh, 2010). The strain was maintained on PDA slants, stored at 4 °C and subcultured periodically.

2.2. Enzyme production

CDA production by *P. oxalicum* SAE_M-51 was carried out under solid-state fermentation (SSF) using mustard oil cake as a solid support. SSF was performed in 250 ml Erlenmeyer flasks by taking appropriate amount of substrate, moistened with fermentation medium (Glucose, 1%; yeast extract, 0.3165%; peptone, 0.4754%; KH_2PO_4, 0.3%; K_2HPO_4, 0.1%; $MgSO_4$, 0.0535%; $(NH_4)_2SO_4$, 0.0255%; NaCl, 0.05% and $CaCl_2$, 0.05%). Following heat sterilization (121 °C, 20 min), the flasks were inoculated with actively growing culture and incubated statically (30 °C, 6 days). After completion of fermentation, appropriate volume of 100 mM borate buffer (pH 9.0) was added to each flask. The extraction of the enzyme was carried out on a rotary shaker (200 rpm) at 4 °C for 1 h. The slurry was squeezed through cheese cloth and the extract was clarified by centrifugation (12,000 × *g*, 4 °C) for 15 min. The clear supernatant was used as the source of enzyme for purification.

2.3. CDA assay

CDA was assayed using ethylene glycol chitin (EGC) as a substrate as described (Kauss & Bausch, 1988).

2.4. Purification of CDA

The crude extracellular enzyme preparation was subjected to three-step purification comprised of ultrafiltration, cation and the anion exchange chromatography. The culture broth was centrifuged at 8000 × *g* for 10 min. The cell free crude enzyme supernatant thus obtained was concentrated using Amicon ultracentrifugal filter unit (10 kDa molecular weight cut-off, Millipore). Concentrated CDA obtained from ultrafiltration was assayed for CDA activity and protein content. Concentrated enzyme thus obtained was loaded on to CM-sepharose (Sigma–Aldrich Co., USA) column equilibrated with borate buffer (100 mM, pH 9.0). The same buffer with a sodium chloride gradient (50–500 mM) was used for elution of protein with a flow rate of 1.0 ml min^{-1}. Fractions were collected and analyzed for CDA activity and protein content. CDA active fractions were pooled, concentrated and further purified using DEAE-sepharose (Sigma–Aldrich Co., USA) column as described above. The active fractions were pooled, concentrated and used for further studies. Bradford (1976) method was used for protein estimation using bovine serum albumin as a standard and sodium dodecyl sulphate-polyacrylamide gel electrophoresis (SDS-PAGE) was performed as described (Laemmli, 1970).

2.5. Zymogram analysis

Native polyacrylamide gel electrophoresis (PAGE) using 10% gel was performed for visualization of enzyme activities in situ as described (Trudel & Asselin, 1990).

2.6. Determination of optimum pH, temperature and stability

The optimum pH for purified CDA was detected by analyzing its activity over a pH range of 4.0–11.0 using the following buffers: 100 mM citrate buffer (4.0–6.0), 100 mM borate buffer (7.0–9.0) and 100 mM carbonate–bicarbonate buffer (10.0–11.0). The stability of enzyme at varying pH was determined by pre-incubating the purified enzyme in the buffers described above for 24 h at 4 °C and subsequently analyzing the residual activity under standard assay conditions.

The optimum temperature was determined by assaying the CDA activity at various temperatures (50–80 °C) for 30 min in 100 mM borate buffer (pH 9.0). The thermostability of enzyme was determined by pre-incubating the enzyme in 100 mM borate buffer (pH 9.0) at various temperatures ranging from 50 to 80 °C. Aliquots were withdrawn at various time intervals, cooled and assayed under standard conditions.

2.7. Thermodynamics of enzyme denaturation

The activation energy ($E_{a,d}$) of the purified CDA was calculated from the slope of Arrhenius plot ($\ln k_d$ vs $1/T$). Free energy (ΔG^*_d), enthalpy (ΔH^*_d) and entropy (ΔS^*_d) of activation for denaturation of the enzyme was calculated using following Eqs. (i)–(iii), respectively. Half-life ($t_{1/2}$) of the enzyme was calculated according to Eq. (iv):

$$\Delta G^*_d = -RT \ln\left(\frac{k_d h}{k_b T}\right) \quad \text{(i)}$$

$$\Delta H^*_d = E_{a,d} - RT \quad \text{(ii)}$$

$$\Delta S^*_d = \frac{\Delta H^*_d - \Delta G^*_d}{T} \quad \text{(iii)}$$

$$t_{1/2} = \ln\frac{2}{k_d} \quad \text{(iv)}$$

where R is the gas constant, h is the Planck constant, k_b is the Boltzmann constant, T is the absolute temperature and k_d is the first-order rate constant calculated from the slope of the regression line obtained by plotting ln relative activity (%) vs time at different temperatures.

2.8. Determination of V_{max}, K_m, K_{cat} and K_{cat}/K_m values

The kinetic parameters of the purified CDA were determined by measuring the enzyme activity at different concentrations (0.5–5 mg ml^{-1}) of *N*-acetyl glucosamine, chitin oligomers (chitobiose, chitotriose, chitopentaose) and glycol chitin. The kinetic constants were then estimated using linear regression plots of Lineweaver and Burk.

2.9. Effect of various metal ions and EDTA on CDA activity

Effect of various mono and bi-valent metal ions (K^+, NH_4^+, Ca^{2+}, Cd^{2+}, Co^{2+}, Cu^{2+}, Zn^{2+}, Mn^{2+}, Mg^{2+}, Fe^{2+}, Ni^{2+}, Li^{2+}, Bi^{2+}, Ba^{2+}, Mo^{2+}, Pb^{2+}) and EDTA on the CDA activity was enumerated by pre-incubating the purified enzyme in the 100 mM borate buffer (pH 9.0) added with an ion (1 mM). After 1 h of incubation, residual activity was measured under standard conditions. The activity assayed in the absence of metal ions was recorded as 100%.

2.10. Acetate inhibition studies

Effect of acetate on CDA activity was determined by assaying the enzyme activity in the presence of various concentrations of acetate (10–100 mM) under standard assay conditions.

2.11. Circular dichroism spectroscopy

Circular dichroism (CD) spectral measurements were performed on a Spectropolarimeter (Chirascan, Applied Photophysics, U.K.). The entire instrument, including the sample chamber, was constantly flushed with N_2 gas during the operation. Far-UV CD spectra (190–240 nm), were recorded in 1 cm path length quartz cell at a protein concentration of 1.0 mg ml^{-1} in buffers (50 mM) of different pH values (HCl–KCl, pH 2; glycine–HCl, pH 4; sodium phosphate, pH 6–8; and glycine–NaOH, pH 9–12). Buffer scans were recorded under the same conditions and subtracted from the protein spectra before further analysis. The results of all the CD measurements were expressed as mean residue ellipticity $[\theta]_\lambda$ in deg cm^2 dmol^{-1} using the relation: $[\theta]_\lambda = \theta_\lambda M_0/10cl$, where θ_λ is the observed ellipticity in millidegrees at wavelength λ, M_0 is the mean residue weight of the protein ($M_0 = 110$), c is the protein concentration (mg/cm^3) and l is the path length (cm). The percentages of different secondary structures (α-helix, β-sheet, turn and random coil) were estimated using K2D2 software (Greenfield, 2007).

2.12. Matrix-assisted laser desorption/ionization time-of-flight (MALDI-TOF/TOF) analysis

For determining the internal peptide sequence through mass spectrometry, the purified protein was first electrophoresed using SDS-PAGE (10%) and was carefully excised. The excised protein band was processed, tryptic digested and peptides obtained were analyzed by MALDI-TOF/TOF (Bruker Daltonics Ultraflex TOF/TOF mass spectrometer, Germany) at proteomics facility of The Center for Genomic Application (TCGA), Okhla Industrial Estate, New Delhi, India. For MALDI-TOF/TOF analysis, the peptide fragments obtained were analyzed with the Flex Analysis Software and database homology search for protein identification was carried out using short sequence BLAST (Basic Local Alignment Search Tool) at NCBI (National Center for Biotechnology Information).

3. Results and discussion

3.1. CDA purification and molecular mass determination

A novel extracellular CDA from *P. oxalicum* SAE$_M$-51 was purified from the crude culture supernatant to homogeneity using ultrafiltration and cation/anion exchange chromatography (Table 1). The purified CDA appeared as a single band with a molecular mass of 53 kDa (Fig. 1). Molecular mass of most of the CDAs purified and studied so far vary in the range of 25–80 kDa (Alfonso, Nuero, Santamaria, & Reyes, 1995; Cai et al., 2006; Nahar et al., 2004). Further, the pI of purified CDA was observed to be 5.2. However, the pI value of CDA from *C. lindemuthianum* (Tokuyasu, Ohnishi-Kameyama, & Hayashi, 1996) and *M. anisopliae* (Nahar et al., 2004) had been detected to vary from 3.7 to 4.1.

3.2. Effect of pH on CDA activity and stability

Purified CDA exhibited maximum activity at pH 9.0, however, notable levels of activity was also detected at pH 6.0. Enzyme stability following analysis had shown that the enzyme retained 100% of its activity at pH 9.0 after 24 h of incubation. Further, it retained about 25–55% of its activity when incubated with buffers of comparatively lower pH of 5.0–7.0. Optimal pH of most of the extracellular CDAs observed so far lies in neutral or alkaline range (Cai et al., 2006; Nahar et al., 2004; Tokuyasu et al., 1996). Further, the optimum pH of intracellular CDA from *M. rouxii* and *A. nidulans* was respectively 5.5 (Kafetzopoulos, Martinou, & Bouriotis, 1993) and 7.0 (Alfonso et al., 1995). In addition, many of the CDAs analyzed so far appeared to be relatively stable at higher pH (Zhao, Park, & Muzzarelli, 2010).

Table 1
Purification profile of chitin deacetylase from *P. oxalicum* SAE$_M$-51.

Purification step	Volume (ml)	Total activity (U)	Total protein (mg)	Specific activity (U mg^{-1})	Yield (%)	Purification fold
Culture supernatant	200	227.79	363.12	0.63	100	1
Ultrafiltration	20	125.70	84.80	1.48	54.87	2.37
CM-sepharose	16.2	72.57	12.38	5.86	31.86	9.34
DEAE-sepharose	18	21.6	0.39	55.38	11.06	88.25

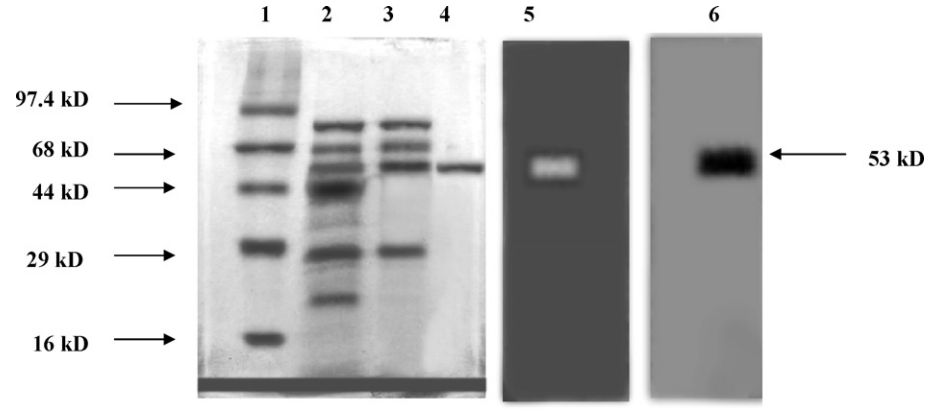

Fig. 1. SDS-polyacrylamide gel and zymogram analysis of purified chitin deacetylase from *P. oxalicum* SAE$_M$-51. Lane 1: protein molecular weight markers; lane 2: crude extract; lane 3: fraction obtained after CM-sepharose purification; lane 4: purified CDA following DEAE-sepharose exchange; lane 5 and 6: zymography of purified CDA after incubation of overlay gels containing 0.1% (w/v) glycol chitin and following staining with Calcofluor white M2R or by treating with nitrous acid before staining.

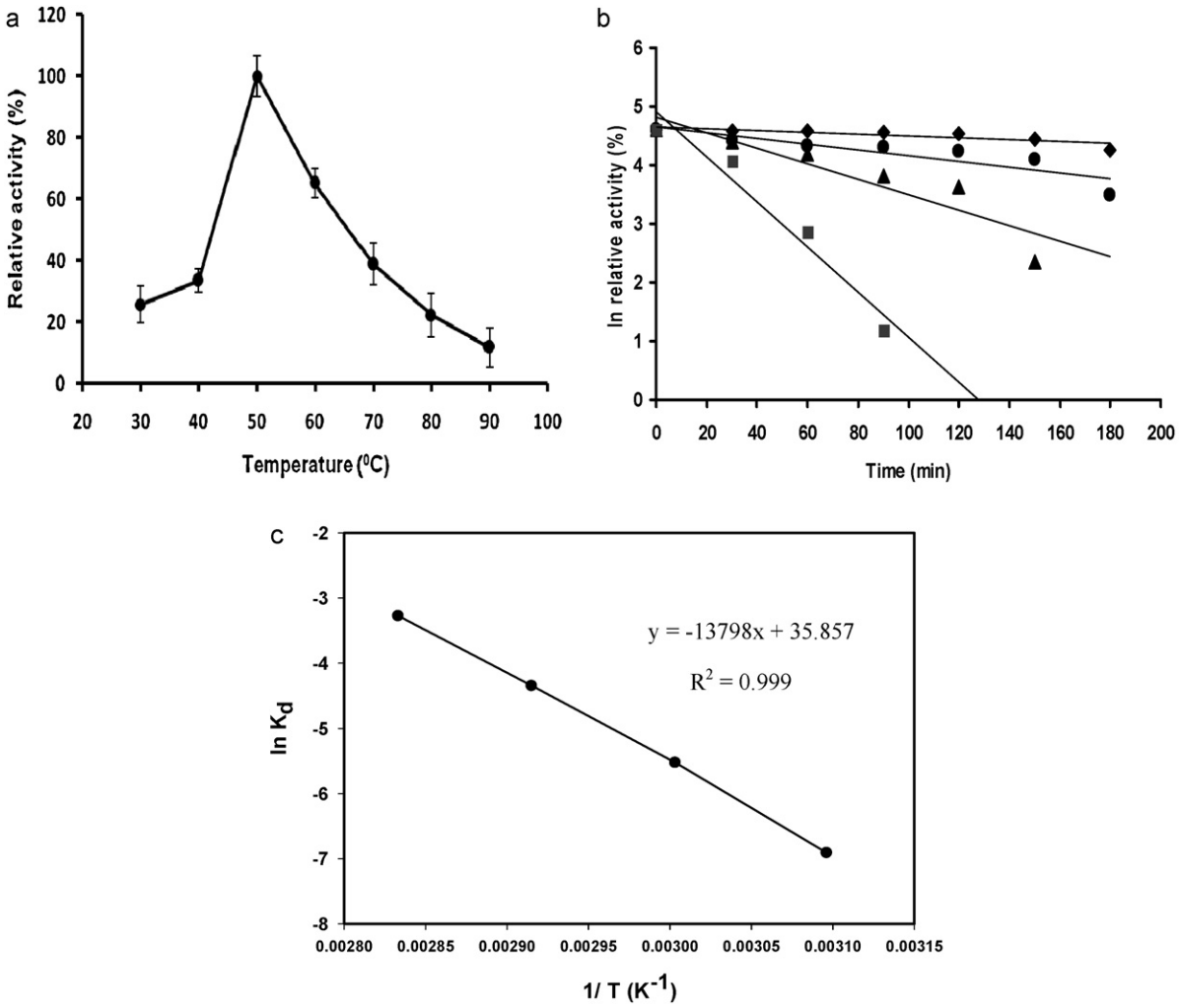

Fig. 2. Effect of temperature (a), pseudo first-order plot (♦, 50 °C; ●, 60 °C; ▲, 70 °C; ■, 80 °C) (b) and Arrhenius plot (c) for thermal denaturation of chitin deacetylase from *P. oxalicum* SAE_M-51.

3.3. Effect of temperature on CDA activity and stability

3.3.1. Kinetics of catalysis

The purified CDA exhibited optimal activity at 50 °C. Enzyme activity reduced when the same was assayed at either lower or higher temperature (Fig. 2a). Thermostability of the enzyme was evaluated by studying the time dependent thermal inactivation of enzyme at various temperatures (50–80 °C). It was observed that the enzyme retained its activity at a wide range of temperature (40–70 °C) (Fig. 2b). Half-life of the enzyme at its optimum temperature was 693.10 min. Optimum temperature of many of the CDAs known so far is around 50 °C (Cai et al., 2006; Kim et al., 2008). CDA from *C. lindemuthianum* DSM 63144 exhibited remarkable thermostability at its optimum temperature with almost no loss of activity after preincubation at 50 °C for 45 h (Tsigos & Bouriotis, 1995). Further, the enzyme from the *A. nidulans* was found to be quite stable over a broad range of (30–100 °C) temperature (Alfonso et al., 1995). The CDA from *C. lindemuthianum* UPS9 had the optimum activity at 60 °C and >50% of the activity was retained after heating of the enzyme at 80 °C for 1 h or at 90 °C for 30 min (Shrestha, Blondeau, Stevens, & Hegarat, 2004).

3.3.2. Thermodynamics of CDA denaturation

Stability of the purified enzyme against thermal denaturation can be articulated by studying its thermodynamic parameters. Thermal denaturation of enzymes is a two step process, which proceeds via formation of an intermediate transition state (U*) which can be refolded into active conformation upon cooling. Complete inactivation of enzymes requires an input of minimum amount of energy i.e. activation energy of denaturation ($E_{a,d}$), which can be calculated by Arrhenius plot ($\ln k_d$ vs $1/T$). The first-order rate constants (k_d) for thermal denaturation of *P. oxalicum* CDA were determined from the slopes of first-order plots (ln relative activity (%) vs time). The values of k_d at 323, 333, 343, and 353 K were 0.001, 0.004, 0.013 and 0.038 min^{-1}, respectively (Fig. 2b). Activation energy for irreversible inactivation '$E_{a,d}$' of the CDA was 114.72 kJ mol^{-1} as calculated by Arrhenius plot (Fig. 2c). The thermal inactivation of the enzymes is accompanied by the disruption of non-covalent linkages including hydrophobic interactions and opening up of the enzyme structure with concomitant increase in the enthalpy (ΔH_d^*) and entropy (ΔS_d^*) of activation for denaturation (Sizer, 1943). Free energy, enthalpy and entropy of activation for enzyme denaturation at different temperatures are listed in Table 2a. It is evident from the Table 2a that Gibbs free energy (ΔG_d^*) of activation for enzyme denaturation is temperature dependent and decreased with a concomitant increase in temperature thereby denoting the decreasing stability of enzyme at higher temperatures. No significant change was observed in the enthalpy (ΔH_d^*) of activation for thermal denaturation of CDA with increasing temperature. Entropy (ΔS_d^*) of activation for complete thermal unfolding

Table 2a
Thermodynamic parameters for denaturation of chitin deacetylase from *P. oxalicum* SAE_M-51.

T (K)	$t_{1/2}$ (min)	ΔG_d^* (kJ mol^{-1})	ΔH_d^* (kJ mol^{-1})	ΔS_d^* (J mol^{-1} K^{-1})
323	693.10	97.86	112.04	43.93
333	173.27	97.15	111.95	44.44
343	53.31	96.78	111.87	43.99
353	23.10	96.55	111.79	43.20

of enzyme appeared to be a temperature independent parameter and its positive values implied that the thermal denaturation of the enzyme at higher temperature resulted in an associated increase in disorderliness of the system. Similar studies were also performed for thermal denaturation of adenosine deaminase (Alrokayan, 2002), ribonuclease (Xiong, Liu, Song, & Ji, 2005) and glucoamylase (Riaz, Perveen, Javed, Nadeem, & Rashid, 2007). The thermodynamic analysis of CDA has so far not been performed and the present paper is first report for the same.

3.4. Kinetic parameters

Kinetic parameters viz. K_m, V_{max}, k_{cat} and k_{cat}/K_m and substrate specificity of CDA from *P. oxalicum* SAE_M-51 were determined through Lineweaver–Burk plot using various concentrations (0.5–5 mg ml^{-1}) of five different substrates (glycol chitin, dimeric, trimeric and pentameric forms of GlcNAc and *N*-acetyl glucosamine) (Fig. 3a and b). The enzyme was not able to deacetylate *N*-acetyl glucosamine, but showed marginal activity towards $(GlcNAc)_2$ and $(GlcNAc)_3$. It was highly active for chitin oligomers having degree of polymerization to be more than four (Table 2b). Enzyme exhibited maximum affinity towards $(GlcNAc)_5$ as evident due to its lowest K_m (3.07 mg ml^{-1}) and highest V_{max} (6.76 μmol min^{-1}) values. Values of Michaelis–Menten constant and specificity constant signifies marginal catalytic activity of enzyme towards chitobiose and chitotriose. A simultaneous increase was observed in the enzyme affinity towards oligomers and as to their degree of polymerization. Values of catalytic constant and specificity constant of the enzyme had also followed the similar pattern and had increased along with the degree of polymerization. CDAs from other microbial sources had also exhibited the similar pattern for glycol chitin and chitin oligomers (Tokuyasu et al., 1996; Wang et al., 2009).

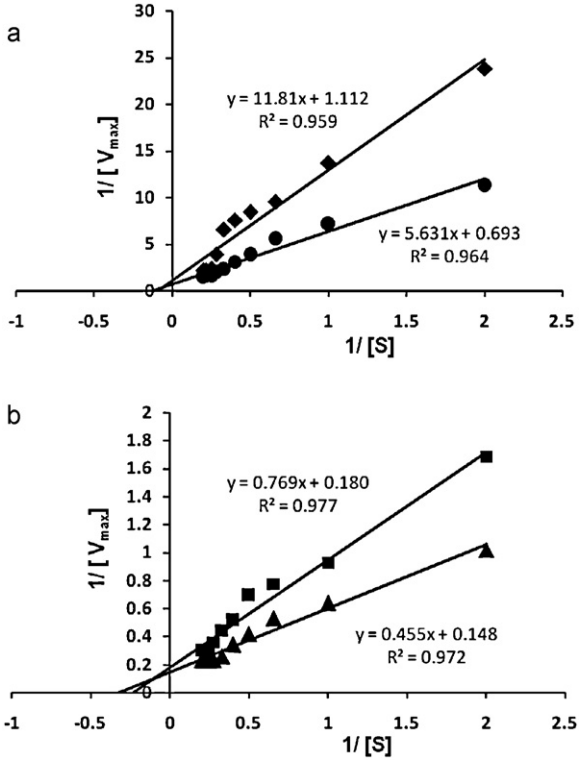

Fig. 3. Double-reciprocal plot for determining the K_m and V_{max} values of chitin deacetylase from *P. oxalicum* SAE_M-51 against chitobiose and chitotriose (a); glycol chitin and chitopentaose (b) (♦, chitobiose; ●, chitotriose; ▲, chitopentaose; ■, glycol chitin).

3.5. Effect of metal ions

CDA activity was assayed in the presence of various metal ions and EDTA. Among the different metal ions studied Cu^{2+}, Co^{2+}, Fe^{2+}, Cd^{2+}, Mg^{2+} and Ca^{2+} appeared as activators of CDA activity and further the enzyme was inhibited by Mo^{2+}, Zn^{2+}, Pb^{2+}, Bi^{2+} and EDTA when added at 1 mM concentrations. Inhibition of CDA activity by EDTA had suggested the enzyme to be a metallo-protein. Previous studies had reported that CDA activity was highly influenced by divalent cations especially cobalt. Catalytic activity of CDA from *S. cerevisiae* could be fully restored by addition of $CoCl_2$ (1 mM). Catalytic ability of CDA from *C. lindemuthianum*, *Mortierella* sp. DY-52 and *Flammulina velutipes* was observed to be enhanced by Zn^{2+}, Ca^{2+} and Co^{2+} (1 mM) (Kim et al., 2008; Shrestha et al., 2004; Yamada et al., 2008). However, Zn^{2+}, Mn^{2+} and Mg^{2+} were found to be inhibitory for CDAs from various sources (Martinou, Koutsioulis, & Bouriotis, 2002).

3.6. Effect of acetate on CDA activity

Sensitivity of enzyme towards end product inhibition was evaluated by assaying the enzyme activity in presence of acetate (0–100 mM). Almost >85% of the enzyme activity was retained in the presence of 0–70 mM sodium acetate and thereafter it declined with a further increase in acetate concentration. Sodium acetate at 80–100 mM had resulted into 30–80% loss in activity; however 50% of the activity was retained at 90 mM concentration. CDA from various microbial sources had distinct end product inhibition kinetics. Most of the fungal CDAs are not inhibited when acetate is present

Table 2b
Substrate specificity and kinetic parameters of chitin deacetylase from *P. oxalicum* SAE_M-51.

Substrate	Relative activity (%)	Kinetic parameters			
		K_m (mg ml^{-1})	V_{max} (μmol min^{-1})	k_{cat} (s^{-1})	k_{cat}/K_m (mg ml^{-1} s^{-1})
Glycol chitin	100	4.27	5.55	231.25	54.16
$(GlcNAc)_2$	16.03	10.62	0.89	37.08	3.49
$(GlcNAc)_3$	25.94	8.13	1.44	60.00	7.38
$(GlcNAc)_5$	121.80	3.07	6.76	281.66	91.75

Table 3
Characteristics of chitin deacetylase at different pH values.

pH	α-Helix (%)	β-Sheet (%)	Random coil (%)
2.0	8.42	17.80	73.78
4.0	14.18	19.24	66.58
6.0	30.56	26.36	43.08
7.0	42.41	28.31	29.28
9.0	56.26	15.63	28.11
10.0	47.13	11.52	58.65
12.0	39.37	5.69	54.94

at lower (1–10 mM) concentrations (Alfonso et al., 1995; Nahar et al., 2004) and inhibition was more pronounced when acetate was present at 40 mM or higher concentrations. A 50% inhibition in CDA activity from *S. cerevisiae* was observed in presence of 40–50 mM of acetate. However, an extracellular CDA from a plant pathogenic fungus *C. lindemuthianum* was not inhibited by sodium acetate even at its higher concentrations (Tokuyasu et al., 1996).

3.7. Circular dichroism spectroscopy

Analysis of the far-UV CD spectra of CDA revealed that the elements of secondary structure are sensitive to the pH of the reaction buffer (Fig. 4). The results suggest that CDA is α, β protein, rather than predominantly β-protein. CDA contains 56.26% α-helix and 15.63% β-structure at its optimal pH (Table 3). The ellipticity values at 222 and 217 nm, characteristic for α-helix and β-sheet conformation, respectively, varied with increasing pH (6, 7, 9, 10, 12) and significantly differ from the values observed at lower pH (2 and 4).

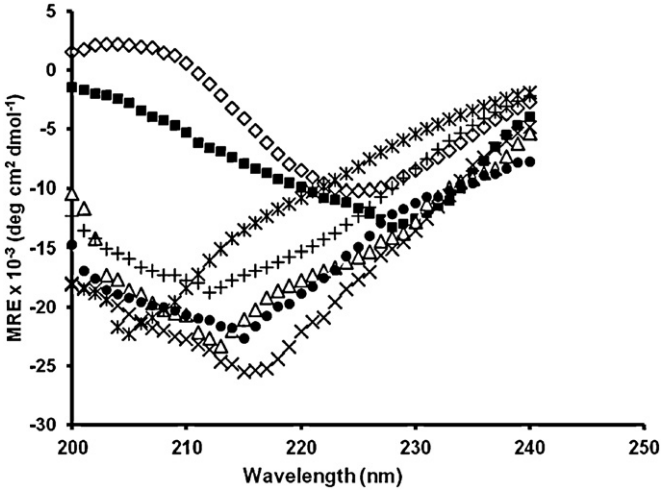

Fig. 4. Far UV-CD spectra of chitin deacetylase from *P. oxalicum* SAE_M-51 as a function of pH (◊, 2; ■, 4; Δ, 6; ×, 7; *, 9; ●, 10; +, 12).

3.8. Determination of internal peptide sequences

The internal amino acid sequencing of CDA was performed by MALDI-TOF/TOF analysis to find out the pattern of homology the enzyme has with other enzymes with deacetylase activity. Enzyme from *P. oxalicum* SAE_M-51 possesses resemblance to members of carbohydrate esterase family 4 that includes

Table 4
Sequence homology of internal peptides of chitin deacetylase from *P. oxalicum* SAE_M-51.

Accession no.	Organism	Sequence	Identity %
Peptide 1	*Penicillium oxalicum*	379 TLQEQEEDVAA 389	–
ZP_07055193.1	*Bacillus cereus*	557 TLQEQEVVNDN 567	54
AAX11701.1	*Rhizopus stolonifer*	87 TSAEVKAAVAA 97	45
AAN65362.1	*Gongronella butleri*	166 FLQEQNLRASM 176	36
Peptide 2	*Penicillium oxalicum*	244 ALTKAAMGGSLE 255	–
YP_002282034.1	*Rhizobium leguminosarum*	223 ALTKAAMAGNGE 234	66
AAT68493.1	*Glomerella lindemuthiana*	09 AAATAALAGSTN 20	42
AAK84438.1	*Blumeria graminis*	102 ALTFDDGPYTSH 113	33
BAI52768.1	*Magnaporthe grisea*	09 AWLAAAALVSAH 20	33
Peptide 3	*Penicillium oxalicum*	329 APLLESLSVKFASPP 343	–
ZP_03502150.1	*Rhizobium etli*	89 APLIERLGIKFESPP 104	47
ACB54958.1	*Helicoverpa armigera*	34 APKKDSLEVELCKDK 48	33
XP_002793041.1	*Paracoccidioides brasiliensis*	224 HQDLESLSAEQRRDQ 238	33
XP_003175982.1	*Arthroderma gypseum*	307 RPLLEIGHDVHEQTV 322	26
Peptide 4	*Penicillium oxalicum*	298 GVGCIDTELLDR 309	–
ZP_06114571.1	*Clostridium hathewayi*	99 GLLKIDTELLDR 110	75
EDN59221.1	*Saccharomyces cerevisiae*	126 GPSASTTKLLDR 137	50
XP_750931.1	*Aspergillus fumigatus*	142 RYTADLLDLLDR 153	33
Peptide 5	*Penicillium oxalicum*	277 STYELLELLTL 287	–
ACF22100.1	*Emericella nidulans*	69 YTEELLEDLAQ 79	54
XP_001394100.1	*Aspergillus niger*	142 YTQDLLDLLDK 152	45
AAW50596.1	*Volvariella volvacea*	196 YTQTLLNLTEA 206	36
Peptide 6	*Penicillium oxalicum*	213 FDVSELWWDRESR 225	–
YP_003343379.1	*Streptosporangium roseum*	206 WDVDTLWRDRDSL 218	54
EEH48938.1	*Paracoccidioides brasiliensis*	370 FSIPGRWWSNTSR 382	38
XP_002911435.1	*Coprinopsis cinerea okayama*	174 NDASRCWWTCGGC 186	31
Peptide 7	*Penicillium oxalicum*	248 AAMGGSLESPIYPRLGGIQ 266	–
ZP_03833676.1	*Pectobacterium cartovorum*	06 AATMYGIESNYPRDLIGYA 24	32
YP_003652570.1	*Thermobispora bispora*	168 AARSHPAVDPERIIVAGIQ 186	32
BAF65669.1	*Vibrio parahaemolyticus*	236 IAMPANSLTEAEPFLGYVD 254	26
YP_003937480.1	*Clostridium sticklandii*	51 FDDGGSEENVKSVLETLDK 69	21

CDAs, rhizobial NodB chitooligosaccharide deacetylase, peptidoglycan *N*-acetylglucosamine deacetylases, acetyl xylan esterases and xylanases A, C, D, E. CDA from *P. oxalicum* SAE_M-51 exhibited significant levels of identity with CDAs of fungal and yeast origin (*Emericella nidulans*, 54%, *Saccharomyces cerevisiae*, 50%; *Rhizopus stolonifer*, 45%). Some of the peptides also showed identity with bacterial deacetylases (*Streptosporangium roseum*, 54%; *Pectobacterium cartovorum*, 32%) (Table 4). Peptide 7 had homology with bacterial CDAs and also showed low level of identity with chitin oligosaccharide deacetylase and acetyl xylan esterase from *Thermobispora bispora* (32%) and *V. parahaemolyticus* (26%).

4. Conclusions

It can be inferred from the present study that chitin deacetylase secreted by *P. oxalicum* SAE_M-51 appears to be a potential candidate for biotechnological production of chitosan. The enzyme was found to be active and stable over a broad range of temperature and pH with high catalytic efficiency and lower inhibition by end products. Results from the thermodynamic studies, far-UV CD spectroscopy and MALDI-TOF/TOF would help understand the complex process of enzyme deactivation, secondary structural elements of the enzyme, its conformational stability and homology with other reported CDAs as well as with members of carbohydrate esterase family 4, respectively. These studies have not been reported so far for the bacterial, yeast and fungal CDAs which in turn may provide additional information about the biochemical and molecular features of the enzyme. A further improvement in the catalytic activity and stability of the enzyme could be achieved by cloning and characterization of the corresponding genes, targeted mutagenesis and deduction of enzyme structural–functional relationships.

Acknowledgements

Senior research fellowship awarded to NP by Council of Scientific and Industrial Research, New Delhi, India and Junior research fellowship awarded to SS by Department of Biotechnology, New Delhi, India are gratefully acknowledged.

References

Alfonso, C., Nuero, O. M., Santamaria, F., & Reyes, F. (1995). Purification of a heat-stable chitin deacetylase from *Aspergillus nidulans* and its role in cell wall degradation. *Current Microbiology*, *30*, 49–54.

Alrokayan, S. (2002). Purification and characterization of adenosine deaminase from camel skeletal muscle. *International Journal of Biochemistry and Cell Biology*, *34*, 1608–1618.

Araki, Y., & Ito, E. (1975). A pathway of chitosan formation in *Mucor rouxii*: Enzymatic deacetylation of chitin. *Biochemical and Biophysical Research Communications*, *56*, 669–675.

Aranaz, I., Mengíbar, M., Harris, R., Paños, I., Miralles, B., Acosta, N., et al. (2009). Functional characterization of chitin and chitosan. *Current Chemical Biology*, *3*, 203–230.

Bradford, M. M. (1976). A rapid and sensitive method for the quantification of microgram quantities of protein utilizing the principle of protein dye binding. *Analytical Biochemistry*, *72*, 248–254.

Cai, J., Yang, J., Du, Y., Fan, L., Qiu, Y., Li, J., et al. (2006). Purification and characterization of chitin deacetylase from *Scopulariopsis brevicaulis*. *Carbohydrate Polymers*, *65*, 211–217.

Caufrier, F., Martinou, A., Dupont, C., & Bouriotis, V. (2003). Carbohydrate esterase family 4 enzymes: Substrate specificity. *Carbohydrate Research*, *338*, 687–692.

Greenfield, N. J. (2007). Using circular dichroism spectra to estimate protein secondary structure. *Nature Protocols*, *1*, 2876–2890.

Kadokura, K., Rokutani, A., Yamamoto, M., Ikegami, T., Sugita, H., Itoi, S., et al. (2007). Purification and characterization of *Vibrio parahaemolyticus* extracellular chitinase and chitin oligosaccharide deacetylase involved in the production of heterodisaccharide from chitin. *Applied Microbiology and Biotechnology*, *75*, 357–365.

Kafetzopoulos, D., Martinou, A., & Bouriotis, V. (1993). Bioconversion of chitin to chitosan: Purification and characterization of chitin deacetylase from *Mucor rouxii*. *Proceedings of the National Academy of Sciences*, *90*, 2564–2568.

Kauss, H., & Bausch, B. (1988). Chitin deacetylase from *Colletotrichum lindemuthianum*. In W. A. Woods, & S. T. Kellogg (Eds.), *Methods in enzymology* (pp. 518–523). Academic Press: San Diego.

Kim, Y.-J., Zhao, Y., Oh, K.-T., Nguyen, V.-N., & Park, R.-D. (2008). Enzymatic deacetylation of chitin by extracellular chitin deacetylase from a newly screened *Mortierella* sp. DY-52. *Journal of Microbiology and Biotechnology*, *18*, 759–766.

Laemmli, U. K. (1970). Cleavage of structural proteins during the assembly of the head of bacteriophage T4. *Nature*, *277*, 680–685.

Martinou, A., Koutsioulis, D., & Bouriotis, V. (2002). Expression, purification and characterization of a cobalt-activated chitin deacetylase (Cda2p) from *Saccharomyces cerevisiae*. *Protein Expression and Purification*, *24*, 111–116.

Maw, T., Tan, T. K., Khor, E., & Wong, S. M. (2002). Selection of *Gongronella butleri* strains for enhanced chitosan yield with UV mutagenesis. *Journal of Biotechnology*, *95*, 189–193.

Nahar, P., Ghormade, V., & Deshpande, M. V. (2004). The extracellular constitutive production of chitin deacetylase in *Metarhizium anisopliae*: Possible edge to entomopathogenic fungi in the biological control of the insect pests. *Journal of Invertebrate Pathology*, *85*, 80–88.

Pareek, N., Vivekanand, V., Dwivedi, P., & Singh, R. P. (2010). Penicillium oxalicum SAE_M-51: A mutagenised strain for enhanced production of chitin deacetylase for bioconversion to chitosan. *New Biotechnology*, *28*, 118–124.

Riaz, M., Perveen, R., Javed, M. R., Nadeem, H., & Rashid, M. H. (2007). Kinetic and thermodynamic properties of novel glucoamylase from *Humicola* sp. *Enzyme and Microbial Technology*, *41*, 558–564.

Shrestha, B., Blondeau, K., Stevens, W. F., & Hegarat, F. L. (2004). Expression of chitin deacetylase from *Colletotrichum lindemuthianum* in *Pichia pastoris*: Purification and characterization. *Protein Expression and Purification*, *38*, 196–204.

Simunek, J., Tishchenko, G., Rozhetsky, K., Bartonova, H., Kopecny, J., & Hodrova, B. (2004). Chitinolytic enzymes from *Clostridium aminovalericum*: Activity screening and purification. *Folia Microbiologica*, *49*, 194–198.

Sizer, I. W. (1943). Effects of temperature on enzyme kinetics. In F. F. Nord, & C. H. Werkman (Eds.), *Advances in enzymology* (pp. 35–62). New York: Interscience Publishers.

Tokuyasu, K., Ohnishi-Kameyama, M., & Hayashi, K. (1996). Purification and characterization of extracellular chitin deacetylase from *Colletotrichum lindemuthianum*. *Bioscience Biotechnology and Biochemistry*, *60*, 1598–1603.

Trudel, J., & Asselin, A. (1990). Detection of chitin deacetylase activity after polyacrylamide gel electrophoresis. *Analytical Biochemistry*, *189*, 249–253.

Tsigos, I., & Bouriotis, V. (1995). Purification and characterization of chitin deacetylase from *Colletotrichum lindemuthianum*. *Journal of Biological Chemistry*, *270*, 26286–26291.

Wang, Y., Song, J.-Z., Yang, Q., Liu, Z.-H., Huang, X.-M., & Chen, Y. (2009). Cloning of a heat-stable chitin deacetylase gene from *Aspergillus nidulans* and its functional expression in *Escherichia coli*. *Applied Biochemistry and Biotechnology*, *162*, 843–854.

Xiong, Y.-H., Liu, J.-Z., Song, H.-Y., & Ji, L.-N. (2005). Purification, kinetic and thermodynamic studies of a new ribonuclease from a mutant of *Aspergillus niger*. *Journal of Biotechnology*, *119*, 348–356.

Yamada, M., Kurano, M., Inatomi, S., Taguchi, G., Mitsuo, M., & Shimosaka, M. (2008). Isolation and characterization of a gene coding for chitin deacetylase specifically expressed during fruiting body development in the basidiomycete *Flammulina velutipes* and its expression in the yeast *Pichia pastoris*. *FEMS Microbiology Letters*, *289*, 130–137.

Zhao, Y., Park, R.-D., & Muzzarelli, R. A. A. (2010). Chitin deacetylases: Properties and applications. *Marine Drugs*, *8*, 24–46.